European Journal of Medicinal Chemistry 102 (2015) 387–397

Contents lists available at ScienceDirect

European Journal of Medicinal Chemistry

journal homepage: http://www.elsevier.com/locate/ejmech

Research paper

Synthesis and in-vitro evaluation of 2-amino-4-arylthiazole as inhibitor of 3D polymerase against foot-and-mouth disease (FMD)

Kwi-wan Jeong [a], Jung-hun Lee [a], Sun-mi Park [a], Joo-Hyung Choi [b], Dae-Youn Jeong [a], Dong-Hwa Choi [a], Yeonju Nam [a], Jong-Hyeon Park [b], Kwang-Nyeong Lee [b], Su-Mi Kim [b, **], Jin-Mo Ku [a, *]

[a] Bio-Center, Gyeonggi Institute of Science and Technology Promotion, 147 Gwanggyo-ro, Yongtong-gu, Suwon-si, Gyeonggi-do, Republic of Korea
[b] Foot-and-Mouth Disease Division, Animal and Plant Quarantine Agency, Ministry of Agriculture, Food and Rural Affairs, 175 Anyangro, Manan-gu, Anyang-si, Gyeonggi-do, Republic of Korea

ARTICLE INFO

Article history:
Received 20 May 2015
Received in revised form
22 July 2015
Accepted 8 August 2015
Available online 12 August 2015

Keywords:
Foot-and-mouth disease virus (FMDV)
Antiviral
Inhibitor
3D polymerase (3Dpol)
2-Amino-4-arylthiazole

ABSTRACT

Foot-and-mouth disease (FMD) is a highly contagious vesicular disease of livestock caused by a highly variable RNA virus, foot-and-mouth disease virus (FMDV). One of the targets to suppress expansion of and to control FMD is 3D polymerase (FMDV 3Dpol). In this study, 2-amino-4-arylthiazole derivatives were synthesized and evaluated for their inhibitory activity against FMDV 3Dpol. Among them, compound **20i** exhibited the most potent functional inhibition (IC_{50} = 0.39 μM) of FMDV 3D polymerase and compound **24a** (EC_{50} = 13.09 μM) showed more potent antiviral activity than ribavirin (EC_{50} = 1367 μM) and T1105 (EC_{50} = 347 μM) with IBRS-2 cells infected by the FMDV O/SKR/2010 strain.

1. Introduction

Foot-and mouth disease (FMD) has been described as the most contagious disease of livestock, such as cattle, sheep, goats and other cloven-hoofed animals [1]. Because of its high morbidity and rapid spread to other animals, outbreaks of FMD have caused severe social and economic losses of stockbreeding [2,3]. The causative agent is foot-and-mouth disease virus (FMDV), a member of the *Aphthovirus* genus in the Picornaviridae family [4]. A total of 7 serotypes (A, O, C, Asia 1 and Southern African Territories (SAT) 1, 2 and 3) and subtypes under the serotypes have been disclosed [5,6]. The FMDV genome is single-stranded RNA that is able to translate a single polyprotein including 4 structural and 10 non-structural proteins [7–9]. The non-structural proteins include 3C protease, for cleaving single polyprotein into functional proteins [10], and 3D polymerase (3Dpol), for carrying out RNA synthesis during transcription and replication [11,12]. From the aspect of a drug target, the variable structural proteins are harnessed to generate specific vaccines; while non-structural proteins such as 3Dpol are used to develop potent antiviral drugs because of their essential role in the viral life cycle.

Though vaccines against FMDV have been developed to control FMD dissemination, they are difficult to control the diverse serotypes and subtypes of FMDV and take at least seven days to trigger immune response against the pathogens after the vaccine is administered, which is called the immunity gap [13–15]. During the past two decades, various efforts have been made to discover and develop antiviral drugs against FMDV. As broad-spectrum replication inhibitors, mutagenic nucleoside analogs such as 5-fluorouracil (FU) [16,17], 5-azacytidine (AZC) [15], 6-azauridine [18], ribavirin (RBV) [19–22] and favipiravir (T-705) [23] and its derivatives have been found to have an anti-FMDV effect. Among them, T-1105 [21,24], a favipiravir derivative, appears to have promise against FMD in spite of its high dose (200–400 mg/kg/day) because it showed significant improvements in symptoms and clinical signs of FMDV-infected pig and guinea pig models [25]. It was also reported that several non-nucleoside compounds inhibited 3Dpol at about 10 μM, of which a pyrimidyl thiophene

* Corresponding author.
** Corresponding author.
E-mail addresses: beliefsk@korea.kr (S.-M. Kim), medichem@gstep.re.kr (J.-M. Ku).

http://dx.doi.org/10.1016/j.ejmech.2015.08.020
0223-5234/

compound, 5D9, had an antiviral effect on FMDV-infected cells [26,27]. As well, several other compounds targeting 3C protease exhibited an anti-FMDV effect [28]; however, there are currently no approved antivirals for the treatment or prevention of FMD.

Herein, we report the screening and synthesis of 2-amino-4-arylthiazole derivatives and an in vitro evaluation of the structure–activity relationship (SAR). The derivatives of 2-amino-4-arylthiazole showed improvements in efficacy, metabolic stability and more potent antiviral activity than reference compounds (T1105, ribavirin) with IBRS-2 cells infected by the FMDV O/SKR/2010 strain, which provoked a nationwide disaster in the Republic of Korea in 2010.

2. Results and discussion

To find hit compounds inhibiting 3Dpol of FMDV, 50,000 compounds stored in the chemical library of the Bio-Center in Gyeonggi Institute of Science Technology Promotion (GSTEP) were screened by high throughput screening (HTS) adapting fluorescence polarization (FP) [29].

FP is a homogeneous method to allow rapid and quantitative analysis of dynamic interactions involving the target enzyme (3Dpol), substrate (PETE, polymerase elongation template element) and compounds. From the HTS campaign, 13 compounds were shown to hamper enzyme–substrate interaction at low μM range, and these were clustered into 2 kinds of hit series and 5 singletones according to their chemical structure (Fig. 1). For hit validation of these compounds, their enzyme inhibitory activities were further evaluated with a functional luciferase assay, by which the byproduct pyrophosphate could be quantified to show the result of RNA polymerization [24]. Cytotoxic molecules were removed by cell counting kit-8 (CCK-8) assay using IBRS-2, a pig kidney cell line. Frequent hitters showing non-specific binding and chemically unstable compounds were also ruled out for final hit validation. Finally, compound **1** was chosen to proceed to chemical modification for structure–activity relationship evaluation.

2.1. Chemistry

For the synthesis of derivatives of compound **1**, convergent synthetic routes were optimized as outlined in Scheme 1. Generally, *N*-substituted-2-amino-4-aryl-thiazole (**9**) was synthesized by reaction of thiourea (**7**) with α-haloacetophenone (**4**) [30]. Diverse thiourea (**7**) was prepared from arylamine (**5**) by two synthetic methods through *N*-acylthiourea (**6**) and isothiocyanate (**8**), respectively. Halogenated acetophenone (**4**) was generated via Friedel-Craft acylation and radical halogenations from corresponding starting-materials (compounds **2** and **3**) [31].

As shown in Scheme 2, compounds **4b**–**h** were generally obtained from aceto compounds **2b**–**h** by the radical halogenation with $CuBr_2$, which were followed by formation of amino thiazole with thioureas (**7a**,**b** and **j**). Compounds **4a** and **7j** are commercially available, which were used without further purification.

Compounds **7a** and **7b** were synthesized from 3- and 4-nitroaniline (**10a** and **10b**) respectively. N-Acetylations of the nitroanilines (**10a** and **10b**) afforded compounds **11a** and **11b**. Nitro reduction of compounds **11a** and **11b** using Pd/C in the presence of H_2 afforded compounds **5a** and **5b**. Next, isothiocyanate formation of compounds **5a** and **5b** by CS_2 and Boc_2O followed by reaction with NH_4OH converted the amino group into thiourea (**7**).

Compounds **19a**–**c** were synthesized through the route as outlined in Scheme 3. Nitro reductions of compound **13** to amine by various conditions (e.g. catalytic hydrogenation, Bechamp reduction and reducing metal reagent ($SnCl_2$)) were examined, however, no desired product was obtained. Alternatively, we chose compound **15** with no need to reduce nitro group as a starting material. After compound **15** was converted to thiourea (**17**), aminothiazole formation of compounds **17** and **4a** gave compound **18**. Deprotection of *N*-Boc of compound **18** afforded compound **14**. Sequentially, amide formation of compound **14** with various acid chlorides provided the corresponding compounds **19a**-**c**.

As outlined in Scheme 4, compounds **7c, d** and **k** as thioureas bearing electron withdrawing groups such as carboxylic acid and cyanide were prepared through the intermediate benzoylthiourea compounds **6c**–**e** that were obtained by reaction of anilines (**5c**–**e**) with benzoyl isothiocyanate. The radical bromination of aceto compounds **2g** and **2h** with $CuBr_2$/EtOAc were performed to provide compound **4g** and **4h**. Alternatively, Friedel–Craft acylation of compounds **3a** and **3b** was carried out using $AlCl_3$ at reflux to afford compounds **4i** and **4j**. Sequentially, aminothiazole formations of compound **4a** and **4g**–**j** were carried out to give compounds **20a**–**k**. Among them, compound **20k** was treated with NaN_3 to provide compound **21** involving tetrazole as a bioisostere of carboxylic acid.

Compounds **24a**–**c** bearing methyl group at R_4 on A ring and R_5 of aminothizole were similarly prepared by thiazole formation of compound **7b** with compounds **23a**–**c**. In addition, structurally rigid compounds **27a**–**b** by the fused ring system were afforded from compounds **26** (Scheme 5).

2.2. Structure–activity relationship (SAR) in target based inhibition test

Primarily, the derivatives of hit compound **1** were designed and synthesized to enhance the inhibitory activity of 3Dpol and to reduce the cytopathic effect to IBRS-2 cells infected by the FMDV O/

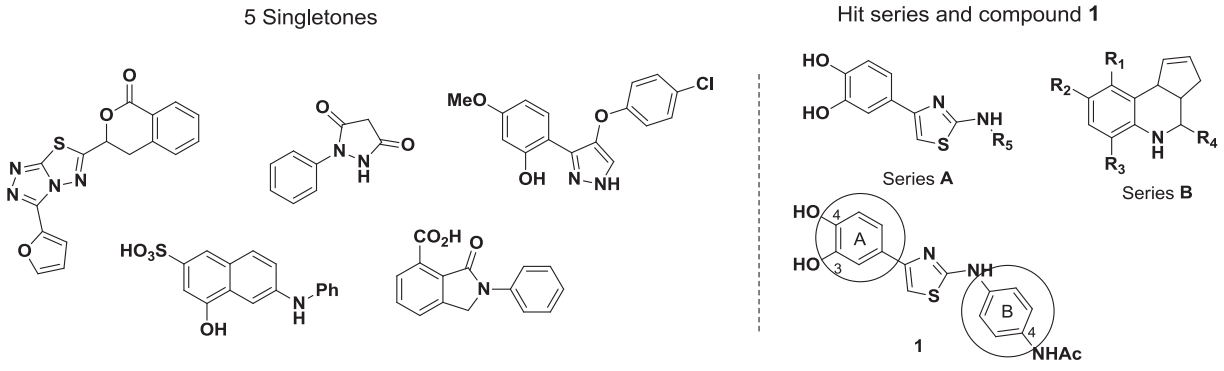

Fig. 1. HTS hits clustering from HTS campaign.

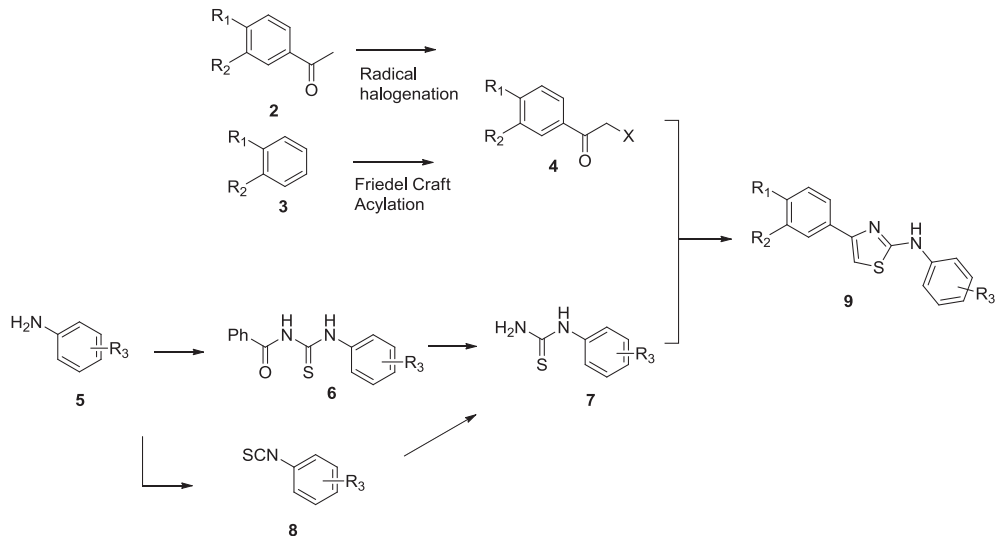

Scheme 1. General synthetic pathway of compound **9** via cyclization of thiourea with haloacetophenones.

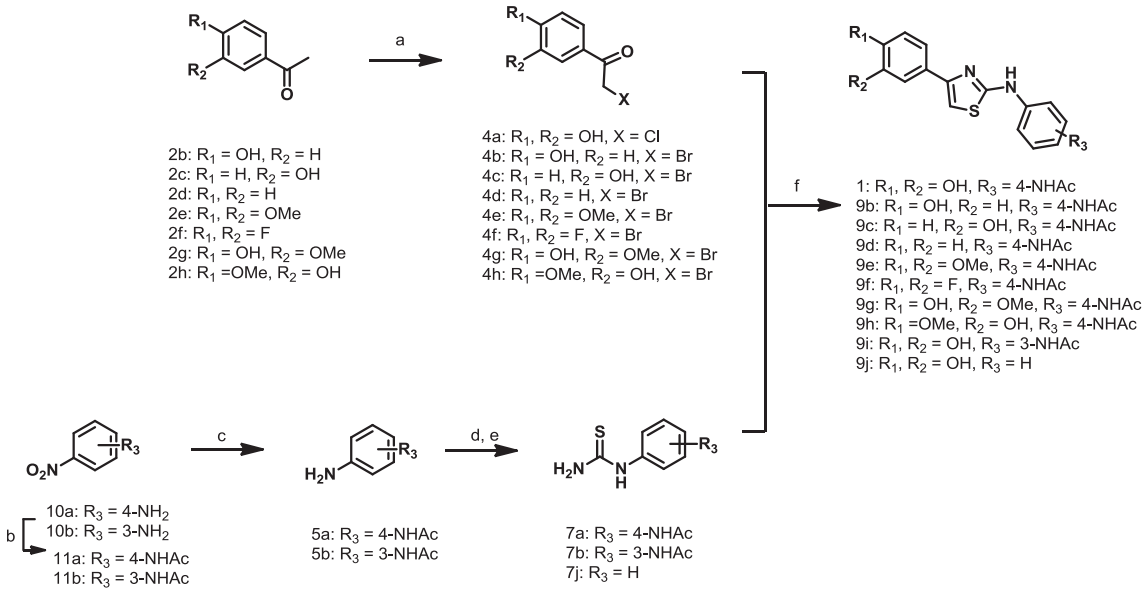

Scheme 2. (a) $CuBr_2$, ethyl acetate, reflux, 2–10 h, 82–99%; (b) acetic anhydride, AcOH, reflux, 70–80%; (c) Pd/C, H_2, MeOH, rt, 8 h, 90–99%; (d) CS_2, TEA, EtOH, rt, 1 h; then Boc_2O, DMAP, 0 °C, 2 h, 90–96%; (e) 7N NH_4 in MeOH, 0 °C to rt, 1 h, 85–97%; (f) EtOH, rt to 80 °C, 1 h–10 h, 70–92%.

SKR/2010 strain. Functional group modifications on the A ring and the B ring of compound **1** (Fig. 1) helped to find the crucial pharmacophores for biological activity. First, we tried to replace the catechol with another functional group along with enzyme activity because catechols may be thought unsuitable in drug discovery due to their low chemical stability and susceptibility to oxidation/reduction even though catechol and quinone derivatives were used in cancer studies [32]. In this study, degradation of compounds **1**, **9i**, **9j** and **19a**–**c** involving catechols was observed in the presence of strong alkali base. It was found that *p*-mono-hydroxylated compounds **9b** and non-substituted compound **9d** showed losses of enzyme activity (Table 1, entry 2 and 4). In addition, there was also a drastic reduction of enzyme activity by compounds **9e** and **9f** (Table 1, entry 5, 6). Therefore, we assumed that hydrogen bonding donor/acceptor relationship and electrostatic effect of the substituents related to inhibition of 3Dpol, which results in the introduction of 4-hydroxy-3-methoxy and 3-methoxy-4-hydroxy on the A ring of compounds **9g** and **9h** respectively (Table 1, entry 7, 8).

Next, we investigated the effect of derivatization of ring B of compound **1** on biological activity such as efficacy, potency and cytotoxicity. Application of catechol in the A ring was able to help in verifying the appropriate functional group in ring B. Compounds **19a**, **19b** and **19c** were able to explain the steric effect of N-substituted amide on the B ring. The smaller acetamide on the B ring (Table 1, entries 1, 11–13) had an advantage for inhibition activity of 3Dpol. Compound **9i**, in which NHAc was substituted on the 3-position instead of the 4-position on the B ring, presented a little enhancement of the inhibition activity of 3Dpol comparing with compound **1** (Table 1, entry 1, 9). The biological assay also examined 3-/4-CO_2H on the B ring as well as inversed carboxamides such as 3-$CONH_2$, 4-$CONH_2$, 3-CONHMe and 4-CONHMe on the B ring (not described here) [33]. Among them, compounds **20a** and **20b** enhanced potency 4–8 fold and showed no cytotoxicity at 200 μM with IBRS-2 cells (Table 1, entry 14, 15).

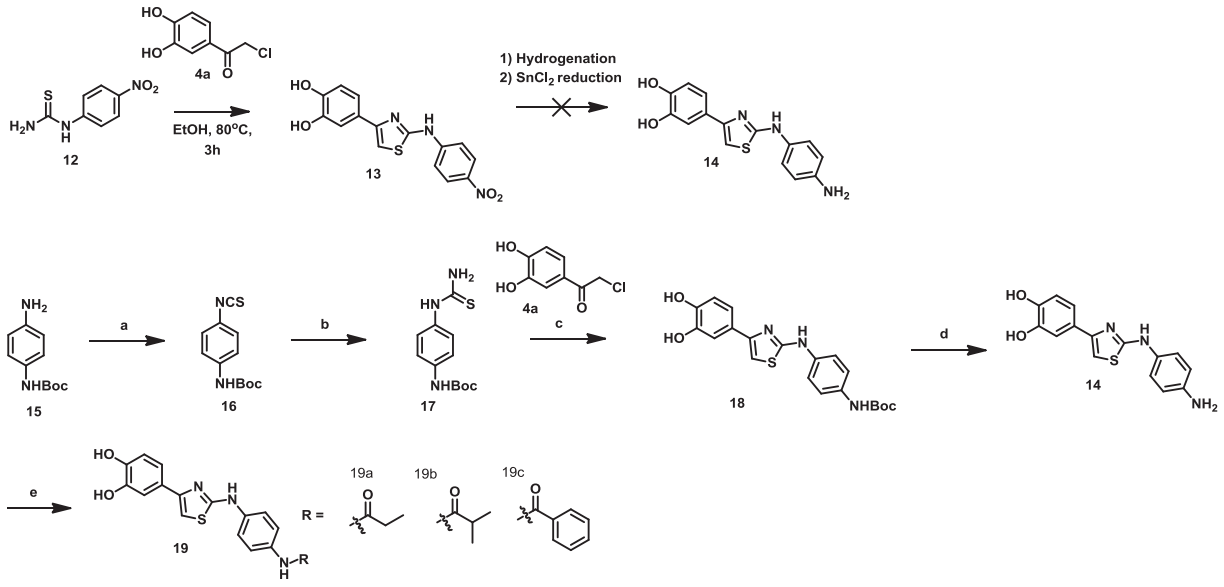

Scheme 3. (a) Thiophosgene, THF, TEA, 0 °C to rt, 83%; (b) 7N NH_4 in MeOH, 0 °C to rt, 1 h, 96%; (c) EtOH, 80 °C, 2 h, 95%; (d) 4N HCl in dioxane, dioxane, 100 °C, 10 h, 97%; (e) acid chloride, TEA, THF, rt, 1–3 h, 62–75%.

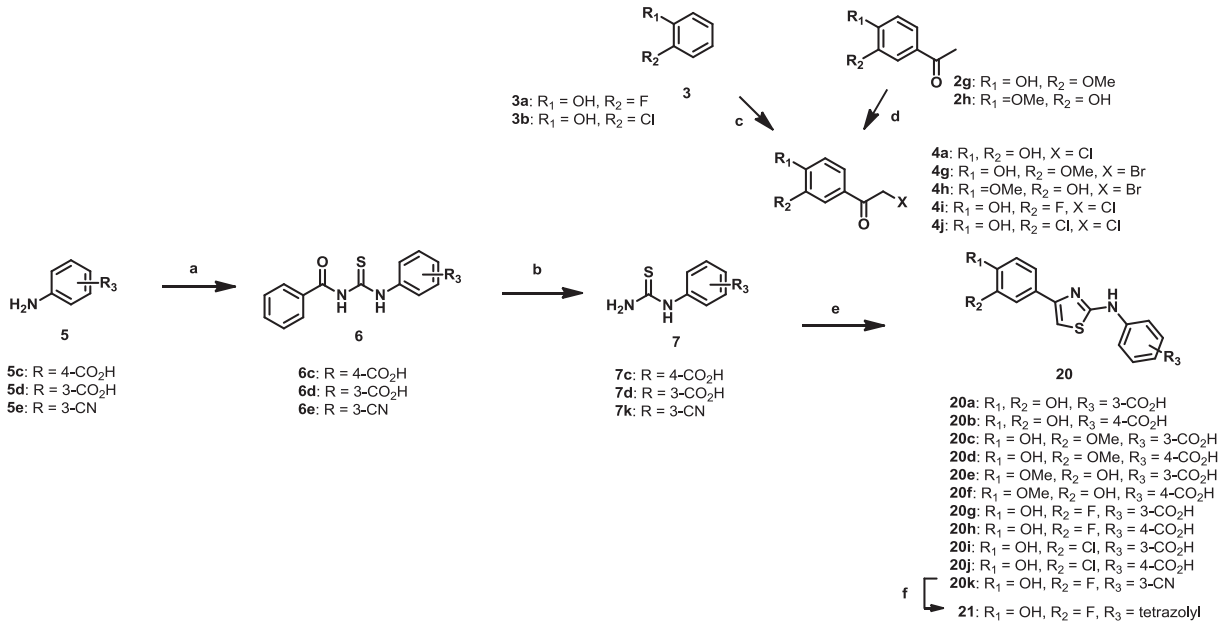

Scheme 4. (a) Benzoyl isothiocyanate, acetone, rt, 1 h, 90–95%; (b) 1N NaOH(aq), THF, reflux, 3 h, 85–91%; (c) chloro acetylchloride, $AlCl_3$, CS_2, reflux, 10 h, 42–65%; (d) $CuBr_2$, ethyl acetate, reflux, 2–10 h, 82–91%; (e) EtOH, rt to 80 °C, 1 h–10 h; (f) NaN_3, DMF, 100 °C, 8 h, 73%.

As described above, functional groups on each side (A, B ring) of compound **1** were combined and introduced. Compounds **20e** and **20f**, which combined 4-OH-3-OMe on the A ring and 3-/4- carboxylic acid on the B ring, had IC_{50}s of 0.79 μM and 1.40 μM respectively and sustained cell viability (Table 1, entry 18, 19). Notably, compounds **20g**, **20h**, **20i** and **20j** (Table 1, entries 20–23), which had F and Cl introduced instead of –OH or -OMe on the meta-position of the A ring, had the highest potency among the 150 compounds synthesized in house. At the initial stage of SAR, we assumed that the hydrogen bonding donor/acceptor relationship and the electrostatic effect of substituent related to inhibition of 3Dpol. However, at the end of SAR, we found that the electrostatic effect is more dominant than hydrogen bonding donor/acceptor relationship. Because the inhibition activities of 3-chloro-4-hydroxy compounds **20i** and **20j** were not significantly different with 3-fluoro-4-hydroxy compounds **20g** and **20h**, and it has been known that fluoride attends a weak hydrogen bonding [34] but chloride does not. A substitution of 3-carboxylic acid into cyanide as a bioisostere on the B ring was applied, Cytotoxicity of compound **20k** was remarkably increased in IBRS-2 cells (CC_{50} = 57.3 μM, not described in Table).

The introductions of 4-methyl on thiazole and 2-methyl-4-hydroxy-3-methoxy on the A ring (i.e. compounds **24a**–**c**) impeded a rotation of the C–C bond between phenyl and thiazole, which showed more potent for the enzyme inhibition (Table 1, entries 26–28). Meanwhile, the ring fused tricyclic compounds **27a** and 27**b** were not significantly effective (Table 1, entries 29–30).

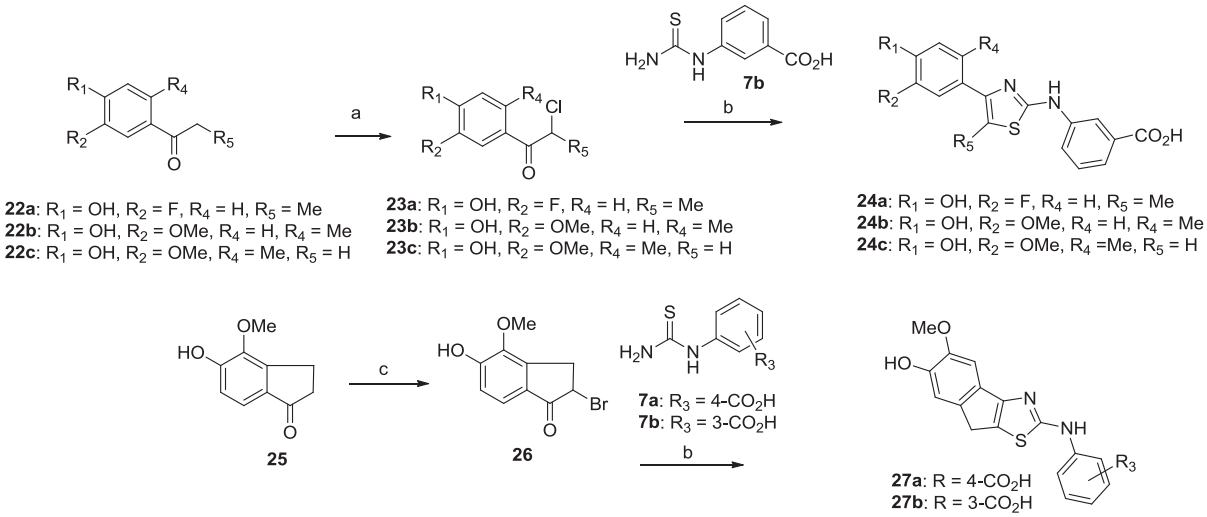

Scheme 5. (a) Propionyl chloride and 2-chloroacetyl chloride, $AlCl_3$, CS_2, reflux, 10 h, 37–54%; (b) EtOH, rt to 80 °C, 1 h–10 h, 81–88%; (c) $CuBr_2$, ethyl acetate, reflux, 6 h, 82%.

Table 1
Enzyme activity and cytotoxicity of derivatives of compound **1**.

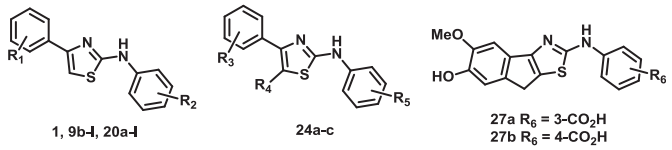

Entry	Compound	R_1	R_2	3Dpol. Inhibition, IC_{50} (μM)
1	**1**	3,4-dihydroxy	4-NHAc	6.8[a]
2	**9b**	4-hydroxy	4-NHAc	NC
3	**9c**	3-hydroxy	4-NHAc	18.3
4	**9d**	H	4-NHAc	NC
5	**9e**	3,4-dimethoxy	4-NHAc	26.4
6	**9f**	3,4-difluoro	4-NHAc	NC
7	**9g**	4-hydroxy-3-methoxy	4-NHAc	3.7
8	**9h**	3-hydroxy-4-methoxy	4-NHAc	7.8
9	**9i**	3,4-dihydroxy	3-NHAc	5.8
10	**9j**	3,4-dihydroxy	H	10.8
11	**19a**	3,4-dihydroxy	4-NHCOEt	9.2
12	**19b**	3,4-dihydroxy	4-NHCOiPr	11.3
13	**19c**	3,4-dihydroxy	4-NHCOPh	32.8
14	**20a**	3,4-dihydroxy	3-CO_2H	0.8[a]
15	**20b**	3,4-dihydroxy	4-CO_2H	1.6[a]
16	**20c**	3-hydroxy-4-methoxy	3-CO_2H	4.1
17	**20d**	3-hydroxy-4-methoxy	4-CO_2H	2.4
18	**20e**	4-hydroxy-3-methoxy	3-CO_2H	0.79[a]
19	**20f**	4-hydroxy-3-methoxy	4-CO_2H	1.4[a]
20	**20g**	3-fluoro-4-hydroxy	3-CO_2H	0.49[a]
21	**20h**	3-fluoro-4-hydroxy	4-CO_2H	2.47[a]
22	**20i**	3-chloro-4-hydroxy	3-CO_2H	0.39[a]
23	**20j**	3-chloro-4-hydroxy	4-CO_2H	1.00[a]
24	**20k**	3-fluoro-4-hydroxy	3-CN	1.43
25	**20l**	3-fluoro-4-hydroxy	3-tetrazolyl	0.63[a]

Entry	Compound	R_3	R_4	R_5	3Dpol. Inhibition, IC_{50} (μM)
26	**24a**	3-fluoro-4-Hydroxy	Me	3-CO_2H	0.57
27	**24b**	4-hydroxy-3-Methoxy	Me	3-CO_2H	0.60
28	**24c**	4-hydroxy-5-Methoxy-2-methyl	H	3-CO_2H	0.54
29	**27a**	Depicted above			1.87
30	**27b**	Depicted above			1.39

[a] No cytotoxicity at 200 μM with IBRS-2 cells using CCK-8.

We observed that compound **1** was readily metabolized in phase I metabolism using minipig liver microsome (Table 2, entry 1). While optimizing the SAR, we verified that the replacement of NHAc into CO_2H (Table 2, entry 1–4) on the B ring enhanced metabolic stability and prolonged half life ($t_{1/2}$) of compound in phase I. Especially, the half life of compound **24a** ($t_{1/2}$ = 1221 min, Table 2, entry 4) was remarkably increased by the modification from compound **1** ($t_{1/2}$ = 19 min, Table 2, entry 1).

Table 2
Metabolic stability of derivatives.

Entry	Compound	Phase I (% remaining)			$t_{1/2}$ (min)
		0 min	30 min	60 min	
1	**1**	100	34.4	17.4	19.0
2	**20b**	100	108.2	102.7	NC
3	**20i**	100	92.6	85.3	256.4
4	**24a**	100	104.4	94.4	1221.0
5	Acetaminophen[a]	100	121.5	123	NC
6	Verapamil[b]	100	4.7	0.8	5.4

[a] Acetoaminophen, positive control, was not metabolized in Phase I.
[b] Verapamil, negative control, was metabolized in Phase I.

2.3. Cell based FMDV inhibition test

We examined the selected compounds by using a functional luciferase assay for 3Dpol inhibition to test the cytopathic effect on IBRS-2 cells infected by the FMDV O/SKR/2010 strain. In this system, compounds were treated for 1 h to IBRS-2 cells infected by 100 $TCID_{50}$ (median tissue culture infective dose) of FMDV. The viral copy number was assessed by real-time PCR, which amplifies and simultaneously detects or quantifies a targeted viral RNA molecule in real time. Effectiveness of a compound as an antiviral was described in terms of the selectivity index (SI, CC_{50}/EC_{50}). High values indicate that the compounds preserved cell viability by reducing the level of the pathogenic virus while lower cytotoxicity was observed.

The compounds **24a** showed relatively low SI values (6.9) comparing with that (21.2) of ribavirin [19,20], a positive control (Table 3, entry 7 and 10). However, compound **24a** (EC_{50} = 13 μM) has an advantage of about 100 fold higher the inhibition activity of 3Dpol than ribavirin (EC_{50} = 1367 μM) to the FMDV O/SKR/2010 strain. In addition, T1105, which has been studied as an antiviral agent for FMDV, are not appropriate for FMDV O/SKR/2010 strain because of low potency and low SI values (EC_{50} = 347 μM, SI = 1.4).

3. Conclusion

FMD is a highly contagious vesicular disease of livestock caused by a highly variable RNA virus, FMDV. One of the targets to suppress expansion of and to control FMD is FMDV 3Dpol. In this study, 2-amino-4-arylthiazole derivatives were synthesized and evaluated for their inhibitory activity against FMDV 3Dpol via a structure–activity relationship. Among them, compound **20i** exhibited the most potent functional inhibition (IC_{50} = 0.39 μM) of 3Dpol in vitro. Also compound **24a** showed moderately potent antiviral activity (EC_{50} = 13.0 μM) as well as SI values (6.9) with IBRS-2 cells infected by the FMDV O/SKR/2010 strain. Though the SI values of compound **24a** (6.9) is relatively lower than ribavirin (21.2), the potency of **24a** (EC_{50} = 13.0 μM) is 100 fold higher than ribavirin (EC_{50} = 1367.0 μM) and 27 fold higher than T1105 (EC_{50} = 346.9 μM) for cell-based FMDV inhibition. In addition, the metabolic stability of compound **24a** ($t_{1/2}$ = 1221 min) is remarkably enhanced, comparing with compound **1** ($t_{1/2}$ = 19 min). Consequently, those compounds represent promising lead compounds for the development of novel antivirals for FMDV as 3Dpol inhibitors. Detailed lead optimization based on DMPK and the physicochemical properties revealed in this work is being carried out in our laboratory.

Table 3
Cell based FMDV inhibition assay (RT-PCR).

Entry	Compound	Cell-based FMDV inhibition assay (RT-PCR)[a]		
		EC_{50} (μM)[b,c]	CC_{50} (μM)[d]	SI (CC_{50}/EC_{50})[e]
1	**1**	142.1 ± 12.6	269.4	1.8
2	**20a**	140.4 ± 11.5	230.7	1.6
3	**20b**	129.4 ± 31.6	394.5	3.1
4	**20i**	144.6 ± 35.8	386.9	2.7
5	**20j**	126.5 ± 8.7	174	1.4
6	**20l**	245.0 ± 49.2	–	–
7	**24a**	13.0 ± 0.4	90.0	6.9
8	**24b**	–	91.1	–
9	**24c**	208.8 ± 0.6	349.5	1.7
10	**Ribavirin**	1367.0 ± 16.9	29070	21.2
11	**T-1105**	346.9 ± 156.6	500	1.4

[a] Compounds were treated for 1 h to IBRS-2 cells infected with 100 $TCID_{50}$[f] of FMDV (FMDV, O/SKR/2010).
[b] EC_{50} is the concentration of a compound that gives half-maximal reduction of viral copy number.
[c] Described by average value ± standard deviation (SD).
[d] The 50% cytotoxic concentration (CC_{50}) was defined as the concentration required to reduce the cell number by 50% compared with that for the untreated controls.
[e] SI: Selectivity index = CC_{50}/EC_{50}.
[f] $TCID_{50}$ is amount of a pathogenic agent that will produce pathological change in 50% of cell cultures inoculated.

4. Experimental section

4.1. 3D polymerase expression and purification

The 3D polymerase (3Dpol) coding sequence of FMDV, O/SKR/5/2010 (Genebank ID: KF112887.1), was cloned in NdeI/SalI multicloning sites of a plasmid pET-21a. Then, it was transformed into the Rosetta2® (DE3) strain (EMD, Millipore). Ampicillin-resistant colonies were grown at 37 °C, followed by induction at OD ~0.9 by the addition of 0.5 mM isopropyl b-D-1-thiogalactopyranoside (IPTG). After additional culture for 4 h, cells were harvested by centrifugation (5000 g, 10 min) and stored at −70 °C. Cell pellets were resuspended in binding buffer (20 mM Hepes, pH 7.4, 350 mM NaCl, 10% glycerol, 40 mM imidazole and 0.1% Tween-20 supplemented with protease inhibitor cocktail) and lysed by sonication using a Sonic Dismembrator (Fischer Scientific). The cleared lysates were subjected to affinity chromatography using Ni sepharose™ high performance resin (GE Healthcare). Elution was conducted using an elution buffer containing the same constituents except the imidazole concentration was 40 mM instead of 500 mM. Fractions containing pure C-terminal hexahistidine-tagged 3Dpol protein (>95%) were pooled and dialyzed against the storage buffer containing 50 mM Hepes pH 7.0, 10% glycerol and 50 mM NaCl. The protein concentration was determined using a Nanodrop spectrophotometer (Thermo Scientific) and coomassie blue staining.

4.2. High throughput screening (HTS) adapting fluorescence polarization

The assay used in the HTS was basically adapted from the polymerase elongation template element (PETE) assay designed by G. Campagnola et al. In brief, 25 μM compounds were pre-incubated with 30 nM 3Dpol for 30 min in a 20 μl assay buffer composed of 50 mM Hepes pH 7.0 and 10% glycerol. Two nanomolar 5′ fluorescein-labeled 8-6 PETE RNA (5′-FAM-UGCAAUGGCCGGCC-GUAAGGCCGGCCA-3′) diluted in 20 μl of the assay buffer was mixed. After 10 min of incubation at room temperature, the total fluorescence and FP signals were measured with an EnVision® microplate reader (Perkin Elmer). The assay plate was a 384-well non-binding black microplate (Greiner). Each screening plate included a negative control panel, PETE RNA alone; a positive control panel, PETE RNA plus 3Dpol and a reference panel, 200 nM of non-labeled PETE RNA. A total of 49,920 compounds selected from the chemical library of the Gyeonggi Bio-center were screened using a JANUS® Automated Workstation (Perkin–Elmer). The

screening data were processed by the Gyeonggi Bio-center Assay Management System (GAMS) derived from Pipeline Pilot protocols (Accelrys). The Z factor ($Z = 1-3(\sigma p + \sigma n)/|\mu p - \mu n|$), where μ and σ are the averages and standard deviations respectively of the FP signals of positive (p) and negative (n) control, was 0.78.

4.3. Functional luciferase inhibition assay

The assay protocol basically followed the previous report by R.C. Durk et al. [9]. The polymerase reactions were carried out in a 384-well white opaque microplate (Greiner). Briefly, 1 μM 3Dpol, 30 μM rUTP and two-fold serially diluted compounds of which the highest concentration was 40 μM were mixed in 20 ul assay buffer containing 25 mM Tris-Cl, pH7.8, 25 mM KCl and 1 mM $MnCl_2$. After pre-incubation at 37 °C for 20 min, the polymerase reaction was initiated by the addition of 5 ul template/primer complexed by heating and cooling of oligo-rA12/oligo-dT18 (1.2 μM/0.12 μM) in the annealing buffer containing 25 mM Tris-Cl pH7.8 and 25 mM KCl. The reactions were allowed to proceed at 37 °C for 1 h. The released pyrophosphate (PPi) was quantified by a PPi-LightTM kit (Lonza) according to the manufacturer's instruction. Luminescence was measured with an EnVision® microplate reader (Perkin Elmer) and IC_{50} was calculated with a Prism® 5 analysis tool (GraphPad Software Inc.).

4.4. Cytotoxicity determination

The porcine kidney IBRS-2 cells were grown in an alpha-minimal essential medium (α-MEM) supplemented with 10% FBS and antibiotics in a 5% CO_2 environment. Cells were seeded in a 384-well black clear bottom microplate at a density of 2500 cells/well. After incubation for 24 h, cells were treated with two-fold serially diluted compounds of which the highest concentration was 200 μM. After incubation for an additional 24 h, cell counting kit 8 (CCK-8) reagent (Dojindo) was added to each well and incubated for 3 h at 37 °C. Absorbance at 470 nm was determined using a Flexstation® 3 microplate reader (Molecular Device). IC_{50} was calculated with a Prism® 5 analysis tool (GraphPad Software Inc.).

4.5. Phase I metabolism assay

Test compounds at 10 μM were mixed with reaction mixture A containing 1 mg/mL minipig liver microsome, 100 mM Tris-Cl (pH7.4), 10 mM glucose-6-phosphate and 0.2 U/mL glucose-6-phosphate dehydrogenase. The reaction was initiated by adding reaction mixture B containing 1 mg/mL nicotinamide adenine dinucleotide phosphate (NADPH) and incubated at 37 °C. At various time points (0, 10, 30 and 60 min), aliquots were removed and added to equal volume of acetonitrile containing 20 μM tolbutamide as an internal standard for reaction termination. After protein precipitation and centrifugation at 12,000 g for 10 min, the supernatant was analyzed by LC-MS/MS. Chromatographic separation was achieved in a run time of 5 min on a C18 column under gradient conditions. Analytes and internal standard were detected by tandem mass spectrometry under positive electrospray ionisation and multiple reaction monitoring (MRM) acquisition mode. All the experiments were performed in duplicate and the percent remaining was calculated by comparing the amount of compounds at each time point with the amount of compounds at time 0 point. The half life (t1/2) was derived by plotting an exponential decay curve using Prism® 5 software (GraphPad). Assay was validated in terms of accuracy and stability by determining the $t_{1/2}$ of verapamil and acetaminophen, which were 5 min and NC (Not calculable), respectively.

4.6. Cells, viruses and virus titration

Swine kidney cells (IBRS-2) were grown in Dulbecco's modified Eagle's medium (D-MEM) supplemented with 10% fetal bovine serum (FBS; pH 7.4) and 1% antibiotics at 37 °C with 5% CO_2. The strain O/SKR/2002 (GenBank accession numbers AY312589 and AY312588), which is one type of FMDV, was used for the viral challenges. Virus titers were determined in IBRS-2 for FMDV. After 3 days, the 50% tissue culture infective dose ($TCID_{50}$) was calculated by the method of Reed and Muench (Reed and Muench, 1938).

4.7. Cell based FMDV inhibition assay and cytotoxicity assay

Assays for inhibition effects and cytotoxicity were performed to determine the effectiveness of antiviral agents for FMDV in IBRS-2 cells. The IBRS-2 cells were plated 1.4×10^4 per well on 96-well plates to be 80% confluent on the well. We used two types of anti-viral agent methods to compare the effectiveness of the chemical compounds. In the first, cells were infected with 100 $TCID_{50}$ FMDV for 1 h and then treated with serially diluted chemical compounds for 48 h (post-treatment). In the second, cells were treated with serially diluted chemical compounds for 18 h and then infected with 100 $TCID_{50}$ FMDV for 1 h (pre-treatment). The cells were incubated at 37 °C and 5% of CO_2 in an incubator for 48 h until the maximum CPE of FMDV was reached. After removing supernatants, the cells were added with an MTS assay solution to detect the level of viability of the infected cells using CellTiter 96 Aqueous One Solution Proliferation Assay (Promega, USA). FMDV inhibition was measured by antiviral activity and cytotoxicity. Antiviral activity was expressed as the 50% effective concentration (EC_{50}), which is defined as the concentration required for reduction of virus-induced cytopathogenicity by 50% of the control value. Cytotoxicity was expressed as the 50% cytotoxic concentration (CC_{50}), which is defined as the concentration required for reduction of cell viability by 50% of the control value. The cytotoxicity assay determined the viability of cells treated with chemical compounds without FMDV infection using CellTiter 96 AQueous One Solution Proliferation Assay (Promega). We calculated selectivity index (SI) values based on the results of OD of CC_{50} and EC_{50} to select effective compounds and concentration ranges.

4.8. Detecting viral RNA of FMDV and analysis in IBRS-2 cells

After 48 h, we collected the supernatant from the cells. Viral RNA was extracted from the supernatant using the MagNa Pure LC 96 System (Roche, Switzerland). Then real-time reverse transcriptase polymerase chain reaction (real-time RT-PCR) was carried out on the extracted RNA to detect the FMDV viral RNA in the cell after treatment of the compounds by the method of Kim et al. [35] T test was performed for statistical analysis using Graph Pad InStat (Ver. 5.0).

4.9. Synthesis and characterization

All commercially available chemicals and reagents were purchased from Aldrich and used without further purification. Melting points were determined with Kruss KSPID apparatus in open capillaries and are uncorrected. The ^1H and ^{13}C NMR spectra were recorded using TMS as the internal standard in DMSO-d_6 or $CDCl_3$ with a Bruker BioSpin GmbH spectrometer at 400 and 600 MHz, respectively. The mass spectra (MS) were recorded on a Thermo Scientific LTQ ORBITRAP instrument with an ESI mass selective detector. Flash column chromatography was performed with silica gel (200–300 mesh) purchased from Merck Co. Ltd.

4.10. General procedure for isothiocyanate

4.10.1. Tert-butyl(4-isothiocyanatophenyl)carbamate (**16**)

To a mixture of tert-butyl-4-aminophenylcarbamate (0.5 g, 2.4 mmol) and triethylamine (0.98 mL, 7.2 mmol) in THF (45 mL) was added dropwise thiophosgene (0.2 mL, 2.64 mmol) at 0 °C, and the mixture was stirred at room temperature for 30 min. The reaction mixture was quenched with water and extracted with ether (2.0×30 mL). The organic layer was dried over Na_2SO_4 and concentrated to give 0.5 g (83%) of the titled compound, which was used for next step without further purification. ^{1}H NMR (400 MHz, $CDCl_3$) δ (ppm) 1.50 (s, 9H), 6.50 (s, 1H), 7.14 (d, J = 8.6 Hz, 2H), 7.34 (d, J = 8.4 Hz, 2H); LRMS (ESI) m/z: 251.2 $[M+H]^+$.

4.11. General procedure 1 for preparation of thiourea (**7**)

4.11.1. Tert-butyl(4-thioureidophenyl)carbamate (**17**)

Tert-butyl(4-isothiocyanatophenyl)carbamate (200 mg, 0.8 mmol) was solubilized in a 7 N solution of NH_3 in MeOH (0.17 ml) and the mixture was stirred for 2 h at room temperature. The solvent was then evaporated and the obtained solid was washed with diethyl ether to give a white powder (206 mg, 96%) that was used in the next reaction step without further purification.

^{1}H NMR (400 MHz, DMSO) δ 9.52 (s, 1H), 9.33 (s, 1H), 7.39 (d, J = 8.8 Hz, 2H), 7.2 (d, J = 8.8 Hz, 2H), 1.47 (s, 9H); LRMS (ESI) m/z: 268.41 $[M+H]^+$.

4.12. General procedure 2 for preparation of thiourea (**7**)

4.12.1. 3-(3-Benzoylthioureido)benzoic acid (**6d**)

To a stirred 3-aminobenzoic acid (1 g, 7.29 mmol) in 15 mL of acetone was added benzoyl isothiocyanate (1.43 g, 8.75 mmol). After being stirred 1 h at room temperature, the mixture was concentrated at reduced pressure, giving a white solid. Recrystallization from ethyl acetate–hexane afforded compound **6d** (2.1 g, 96%) as a pale white solid.

^{1}H NMR (400 MHz, DMSO) δ 12.63 (s, 1H), 11.64 (s, 1H), 8.31 (s, 1H), 8.00–7.98 (d, J = 7.06 Hz, 2H), 7.90–7.83 (m, 2H), 7.67–7.65 (m, 1H), 7.57–7.53 (m, 3H).

4.12.2. 3-Thioureidobenzoic acid (**7d**)

The 3-(3-benzoylthioureido)benzoic acid (1 g, 3.33 mmol) was refluxed in 10 percent NaOH aqueous solution (33 mL) at 100 °C for 1 h. The reaction mixture was cooled and acidified with dilute HCl to get a solid which was filtered and washed with water and dried. The dried solid was further recrystallized in dry ether to yield compound **7d** as pure solid (620 mg, 94.8%).

^{1}H NMR (400 MHz, DMSO) δ 12.98 (s, 1H), 9.83 (s, 1H), 8.02 (s, 1H), 7.69–7.66 (m, 2H), 7.45–7.41 (m, 1H).

4.13. General procedure of 2-amino thiazole formation

The properly substituted bromoacetophenone **4a**–**h** (1 equiv) and thioureas **7a**–**k** (1 equiv) were solubilized in dry ethanol (1 mL/mmol^{-1} of bromoacetophenone) and reacted at rt~70 °C until consumption of the starting materials as indicated by TLC. After cooling, the solvent was evaporated and the obtained residue was washed with diethyl ether (2 × 1 mL) or ethyl acetate (2 × 1 mL) to give the title compounds as a powder in good overall yields. In some cases, the crude material was purified by flash column chromatography.

4.14. General procedure of a-chloroacetylation via Friedel–Craft acylation

4.14.1. 2-Chloro-1-(3-chloro-4-hydroxyphenyl)ethan-1-one (**4j**)

To a cooled (ice bath) stirred solution of 2-chlorophenol (500 mg, 3.89 mmol) in 10 mL of carbon disulfide was continuously added (3.2 g, 24.12 mmol) of anhydrous aluminum chloride portionwise. The stirred, cooled mixture was then treated dropwise with (571 mg, 5.05 mmol) of 2-chloroacetyl chloride. After the addition was completed, the mixture was heated at reflux temperature for 20 h, cooled, and poured into a mixture of crushed ice and 15 ml of concentrated hydrochloric acid. The solid which gradually crystallized was washed with water and carbon disulfide and dried. The solid was recrystallized from diethyl ether to yield compound **4j** as white solid (389 mg, 49%).

4.15. General procedure of a-chloroacetylation via radical bromination

4.15.1. 2-Bromo-1-(4-hydroxyphenyl)ethan-1-one (**4b**)

A mixture of 4-hydroxyacetophenone (500 mg, 3.67 mmol) and copper(II) bromide (902 mg, 4.04 mmol) in ethyl acetate (10 mL) was heated at reflux under N_2 for 5 h. The mixture was filtered through Celite(TM). The filter cake was washed with ethyl acetate, and the combined filtrates were evaporated and then the residue was washed with diethyl ether to afford compound **4b**. ^{1}H NMR (400 MHz, $CDCl_3$) δ 7.92 (d, J = 7.2 Hz, 2H), 6.99 (d, J = 7.2 Hz 2H), 4.41 (s, 2H), 3.85 (s, 1H).

4.15.2. 4-(2-((3-(2H-Tetrazol-5-yl)phenyl)amino)thiazol-4-yl)-2-fluorophenol (**21**)

A mixture of 3-((4-(3-fluoro-4-hydroxyphenyl)thiazol-2-yl) amino)benzonitrile (30 mg, 0.096 mmol), sodium azide (62.6 mg, 0.96 mmol) and ammonium chloride (51.35 mg, 0.96 mmol) in DMF (0.96 mL) was heated for 8 h at 100 °C. The reaction mixture was cooled to room temperature and concentrated, the residue was dissolved in EtOAc (75 mL) and washed with 1N HCl (2 × 30 mL). The organic layer was dried over Na_2SO_4 and concentrated in vacuo. The crude was purified by trituration with hexane/EtOAc (90/10) to afforded compound **21** (25 mg, 73.4%) as a pale yellow solid. ^{1}H NMR (400 MHz, DMSO) δ 10.54 (s, 1H), 10.01 (s, 1H), 8.55 (s, 1H), 7.93–7.88 (m, 1H), 7.72 (dd, J = 12.7, 1.8 Hz, 1H), 7.62 (d, J = 8.4 Hz, 1H), 7.57 (d, J = 6.4 Hz, 2H), 7.27 (s, 1H), 7.00 (t, J = 8.8 Hz, 1H); LRMS (ESI) m/z: 355.1 $[M+H]^+$

4.15.3. N-(4-((4-(3,4-Dihydroxyphenyl)thiazol-2-yl)amino)phenyl) acetamide (**1**)

MP: 216.4 °C; ^{1}H NMR (DMSO-d_6) δ 10.26 (s, 1H), 9.94 (s, 1H), 7.62 (d, J = 8.8 Hz, 2H), 7.56 (d, J = 8.8 Hz, 2H), 7.32 (d, J = 2.0 Hz, 1H), 7.17 (dd, J = 6.4 Hz, J = 2.0 Hz, 1H), 6.95 (s, 1H), 6.77 (d, J = 8.0 Hz, 1H), 1.91 (s, 3H); ^{13}C NMR (100 MHz, DMSO) δ 168.25, 163.28, 151.00, 145.56, 137.31, 133.58, 126.93, 120.29, 120.19, 117.57, 117.52, 116.15, 113.92, 99.88, 24.33; LRMS (ESI) m/z: 342.1 $[M+H]^+$; HRMS (ESI) m/z: Calcd. for $[M+H]^+$ $C_{17}H_{16}N_3O_3S$: 342.0907; found: 342.0905.

4.15.4. N-(4-(4-(4-Hydroxyphenyl)thiazol-2-ylamino)phenyl) acetamide (**9b**)

MP: 220.3 °C; ^{1}H NMR (400 MHz, DMSO) δ 10.11 (s, 1H), 9.84 (s, 1H), 9.54 (s, 1H), 7.73 (d, J = 8.7 Hz, 2H), 7.62 (d, J = 9.0 Hz, 2H), 7.52 (d, J = 9.1 Hz, 2H), 2.02 (s, 3H); ^{13}C NMR (175 MHz, DMSO) δ 168.24, 163.50, 157.52, 150.83, 137.28, 133.63, 127.55, 126.48, 120.34, 117.63, 115.80, 99.88, 24.34; LRMS (ESI) m/z: 326.1 $[M+H]^+$; HRMS (ESI) m/z: Calcd. for $[M+H]^+$ $C_{17}H_{16}N_3O_2S$: 326.0958; found: 326.0959.

*4.15.5. N-(4-((4-(3-Hydroxyphenyl)thiazol-2-yl)amino)phenyl) acetamide (**9c**)*

MP: 201.3 °C; ^{1}H NMR (400 MHz, DMSO) δ 10.17 (s, 1H), 9.86 (s, 1H), 7.66–7.60 (m, 2H), 7.54 (d, J = 8.9 Hz, 2H), 7.36–7.30 (m, 2H), 7.23–7.17 (m, 2H), 6.70 (dd, J = 7.9, 1.6 Hz, 1H), 2.03 (s, 3H); ^{13}C NMR (100 MHz, DMSO) δ 168.26, 163.48, 158.00, 150.65, 137.20, 136.30, 133.71, 130.02, 120.30, 117.67, 116.91, 115.04, 113.17, 102.87, 24.34; LRMS (ESI) *m/z*: 326.1 $[M+H]^+$; HRMS (ESI) *m/z*: Calcd. for $[M+H]^+$ $C_{17}H_{15}N_3O_2S$: 326.0958; found: 326.0955.

*4.15.6. N-(4-((4-Phenylthiazol-2-yl)amino)phenyl)acetamide (**9d**)*

MP: 286.4 °C; ^{1}H NMR (400 MHz, DMSO) δ 10.19 (s, 1H), 9.85 (s, 1H), 7.91 (d, J = 8.2 Hz, 2H), 7.63 (d, J = 9.0 Hz, 2H), 7.54 (d, J = 8.2 Hz, 2H), 7.43 (t, J = 7.7 Hz, 2H), 7.33–7.28 (m, 2H), 2.02 (s, 3H); ^{13}C NMR (100 MHz, DMSO) δ 168.39, 162.58, 147.54, 136.41, 134.34, 133.94, 129.12, 128.81, 128.42, 126.24, 120.35, 118.21, 103.12, 90.10, 24.33; LRMS (ESI) *m/z*: 310.1 $[M+H]^+$; HRMS (ESI) *m/z*: Calcd. for $[M+H]^+$ $C_{17}H_{16}N_3OS$: 310.1009; found: 310.1011.

*4.15.7. N-(4-((4-(3,4-Dimethoxyphenyl)thiazol-2-yl)amino)phenyl) acetamide (**9e**)*

MP: 231.4 °C; ^{1}H NMR (400 MHz, DMSO) δ 10.15 (s, 1H), 9.84 (s, 1H), 7.60 (d, J = 9.0 Hz, 2H), 7.53 (d, J = 9.1 Hz, 2H), 7.50–7.44 (m, 2H), 7.18 (s, 1H), 7.01 (d, J = 8.4 Hz, 1H), 3.83 (s, 3H), 3.78 (s, 3H), 2.02 (s, 3H); ^{13}C NMR (100 MHz, DMSO) δ 168.25, 163.57, 150.51, 149.16, 148.96, 137.22, 133.73, 128.16, 120.37, 118.84, 117.76, 112.27, 109.81, 101.08, 55.96, 55.93, 24.32; LRMS (ESI) *m/z*: 370.1 $[M+H]^+$; HRMS (ESI) *m/z*: Calcd. for $[M+H]^+$ $C_{19}H_{20}N_3O_3S$: 370.1220; found: 370.1219.

*4.15.8. N-(4-((4-(3,4-Difluorophenyl)thiazol-2-yl)amino)phenyl) acetamide (**9f**)*

MP: 204.6 °C; ^{1}H NMR (400 MHz, DMSO) δ 10.22 (s, 1H), 9.85 (s, 1H), 7.93 (dd, J = 12.2, 7.9, 2.1 Hz, 1H), 7.81–7.75 (m, 1H), 7.61 (d, J = 9.0 Hz, 2H), 7.54 (d, J = 9.0 Hz, 2H), 7.49 (dt, J = 10.5, 8.6 Hz, 1H), 7.40 (s, 1H), 2.02 (s, 3H); ^{13}C NMR (100 MHz, DMSO) δ 168.27, 163.96, 151.35, 148.36, 148.10, 136.96, 133.89, 132.70, 122.92, 120.36, 118.22 (d, J = 17 Hz) 118.14, 117.86, 114.85 (d, J = 19 Hz), 104.15, 24.33; LRMS (ESI) *m/z*: 346.1 $[M+H]^+$; HRMS (ESI) *m/z*: Calcd. for $[M+H]^+$ $C_{17}H_{14}F_2N_3OS$: 346.0820; found: 346.0818.

*4.15.9. N-(4-((4-(4-Hydroxy-3-methoxyphenyl)thiazol-2-yl)amino) phenyl)acetamide (**9g**)*

MP: 218.9 °C; ^{1}H NMR (400 MHz, DMSO) δ 10.12 (s, 1H), 9.84 (s, 1H), 7.60 (d, J = 9.0 Hz, 2H), 7.52 (d, J = 9.1 Hz, 2H), 7.43 (d, J = 1.9 Hz, 1H), 7.35 (dd, J = 8.2, 1.8 Hz, 1H), 7.08 (s, 1H), 6.81 (d, J = 8.2 Hz, 1H), 3.84 (s, 3H), 2.02 (s, 3H); ^{13}C NMR (100 MHz, DMSO) δ 168.24, 163.47, 150.87, 148.02, 146.85, 137.26, 133.67, 126.89, 120.37, 119.21, 117.71, 115.99, 110.28, 100.23, 56.05, 24.32; LRMS (ESI) *m/z*: 356.1 $[M+H]^+$; HRMS (ESI) *m/z*: Calcd. for $[M+H]^+$ $C_{18}H_{18}N_3O_3S$: 356.1063; found: 356.1066.

*4.15.10. N-(4-((4-(3-Hydroxy-4-methoxyphenyl)thiazol-2-yl) amino)phenyl)acetamide (**9h**)*

MP: 215.6 °C; ^{1}H NMR (400 MHz, DMSO) δ 10.12 (s, 1H), 9.86 (s, 1H), 7.62 (d, J = 8.9 Hz, 2H), 7.57–7.50 (m, 2H), 7.35 (s, 1H), 7.31 (d, J = 8.4 Hz, 1H), 7.03 (s, 1H), 6.95 (d, J = 8.4 Hz, 1H), 3.79 (s, 3H), 2.02 (s, 3H); ^{13}C NMR (100 MHz, DMSO) δ 168.24, 163.38, 150.61, 147.84, 146.85, 137.26, 133.64, 128.32, 120.29, 117.61, 117.26, 113.69, 112.69, 100.75, 56.07, 24.33; LRMS (ESI) *m/z*: 356.1 $[M+H]^+$; HRMS (ESI) *m/z*: Calcd. for $[M+H]^+$ $C_{18}H_{18}N_3O_3S$: 356.1063; found: 356.1066.

*4.15.11. N-(3-((4-(3,4-Dihydroxyphenyl)thiazol-2-yl)amino) phenyl)acetamide (**9i**)*

MP: 224.9 °C; ^{1}H NMR (400 MHz, DMSO) δ 10.24 (s, 1H), 9.97 (s, 1H), 7.89 (d, J = 1.8 Hz, 1H), 7.56 (d, J = 8.1 Hz, 1H), 7.32 (t, J = 2.0 Hz, 1H), 7.26–7.20 (m, 2H), 7.12 (s, 1H), 6.96 (s, 1H), 6.76 (dd, J = 8.2, 1.7 Hz, 1H), 2.06 (s, 3H); ^{13}C NMR (100 MHz, DMSO) δ 168.75, 163.13, 151.06, 145.68, 145.57, 142.06, 140.30, 129.57, 126.93, 117.81, 116.07, 113.90, 112.52, 112.13, 108.02, 100.30, 24.57; LRMS (ESI) *m/z*: 342.1 $[M+H]^+$; HRMS (ESI) *m/z*: Calcd. for $[M+H]^+$ $C_{17}H_{15}N_3O_3S$: 342.0907; found: 342.0908.

*4.15.12. 4-(2-(Phenylamino)thiazol-4-yl)benzene-1,2-diol (**9j**)*

MP: 244.8 °C; ^{1}H NMR (400 MHz, DMSO) δ 9.94 (s, 1H), 7.40 (s, 2H), 7.03 (s, 2H), 6.88 (s, 1H), 6.66 (s, 1H), 6.46 (s, 1H); ^{13}C NMR (100 MHz, DMSO) δ 164.33, 148.68, 146.17, 145.73, 141.04, 129.64, 125.39, 122.69, 118.23, 117.71, 116.28, 114.04, 100.33; LRMS (ESI) *m/z*: 285.1 $[M+H]^+$; HRMS (ESI) *m/z*: Calcd. for $[M+H]^+$ $C_{15}H_{13}N_2O_2S$: 285.0692; found: 285.0690.

*4.15.13. N-(4-((4-(3,4-Dihydroxyphenyl)thiazol-2-yl)amino) phenyl)propionamide (**19a**)*

MP: 209.1 °C; ^{1}H NMR (400 MHz, DMSO) δ 10.07 (s, 1H), 9.76 (s, 1H), 8.99 (s, 1H), 7.62 (d, J = 8.9 Hz, 1H), 7.54 (d, J = 9.0 Hz, 2H), 7.32 (d, J = 2.0 Hz, 1H), 7.18 (dd, J = 8.2, 2.1 Hz, 1H), 6.93 (s, 1H), 6.76 (d, J = 8.2 Hz, 1H), 2.30 (q, J = 15.3, 7.7 Hz, 2H), 1.09 (t, J = 7.6 Hz, 3H); ^{13}C NMR (100 MHz, DMSO) δ 171.97, 163.30, 151.00, 145.65, 145.56, 137.24, 133.64, 126.94, 120.31, 117.60, 117.52, 116.14, 113.92, 99.86, 29.90, 10.28; LRMS (ESI) *m/z*: 356.1 $[M+H]^+$; HRMS (ESI) *m/z*: Calcd. for $[M+H]^+$ $C_{18}H_{18}N_3O_3S$: 356.1063; found: 356.1066.

*4.15.14. N-(4-((4-(3,4-Dihydroxyphenyl)thiazol-2-yl)amino) phenyl)isobutyramide (**19b**)*

MP: 213.4 °C; ^{1}H NMR (400 MHz, DMSO) δ 10.07 (s, 1H), 9.73 (s, 1H), 8.99 (s, 2H), 7.61 (d, J = 9.1 Hz, 2H), 7.56 (d, J = 9.1 Hz, 2H), 7.32 (d, J = 2.1 Hz, 1H), 7.18 (dd, J = 8.2, 2.1 Hz, 1H), 6.93 (s, 1H), 6.80–6.74 (m, 1H), 2.57 (dt, J = 13.6, 6.8 Hz, 2H), 1.10 (d, J = 6.8 Hz, 5H); ^{13}C NMR (175 MHz, DMSO) δ 175.21, 163.35, 151.02, 145.68, 145.59, 137.27, 133.71, 126.96, 120.46, 117.63, 117.55, 116.15, 113.94, 99.89, 35.28, 20.07; LRMS (ESI) *m/z*: 370.1 $[M+H]^+$; HRMS (ESI) *m/z*: Calcd. for $[M+H]^+$ $C_{19}H_{20}N_3O_3S$: 370.1220; found: 370.0817.

*4.15.15. N-(4-((4-(3,4-Dihydroxyphenyl)thiazol-2-yl)amino) phenyl)benzamide (**19c**)*

MP: 234.9 °C; ^{1}H NMR (400 MHz, DMSO) δ 10.17 (d, J = 14.3 Hz, 2H), 9.01 (d, J = 3.6 Hz, 2H), 7.98–7.92 (m, 2H), 7.77–7.66 (m, 4H), 7.60–7.50 (m, 3H), 7.34 (d, J = 2.1 Hz, 1H), 7.20 (dd, J = 8.2, 2.1 Hz, 1H), 6.96 (s, 1H), 6.77 (d, J = 8.2 Hz, 1H); ^{13}C NMR (100 MHz, DMSO) δ 165.63, 163.22, 151.03, 145.68, 145.58, 137.88, 135.59, 133.24, 131.85, 128.82, 128.03, 126.93, 121.73, 117.54, 117.42, 116.16, 113.93, 100.02; LRMS (ESI) *m/z*: 403.1 $[M+H]^+$; HRMS (ESI) *m/z*: Calcd. for $[M+H]^+$ $C_{22}H_{18}N_3O_3S$: 404.1063; found: 404.1064.

*4.15.16. 3-((4-(3,4-Dihydroxyphenyl)thiazol-2-yl)amino)benzoic acid (**20a**)*

MP: 297.4 °C; ^{1}H NMR (400 MHz, DMSO) δ 10.42 (s, 1H), 8.25 (s, 1H), 8.07 (d, J = 8.0 Hz, 1H), 7.57–7.41 (m, 2H), 7.31 (d, J = 2.1 Hz, 1H), 7.22 (dd, J = 8.2, 2.0 Hz, 1H), 7.02 (s, 1H), 6.77 (d, J = 8.2 Hz, 1H); ^{13}C NMR (100 MHz, DMSO) δ 168.08, 162.85, 151.05, 145.76, 145.62, 141.90, 132.47, 129.62, 126.83, 122.20, 120.93, 117.96, 117.71, 116.07, 113.88, 100.72; LRMS (ESI) *m/z*: 329.1 $[M+H]^+$; HRMS (ESI) *m/z*: Calcd. for $[M+H]^+$ $C_{16}H_{13}N_2O_4S$: 329.0591; found: 329.0592.

*4.15.17. 4-((4-(3,4-Dihydroxyphenyl)thiazol-2-yl)amino)benzoic acid (**20b**)*

MP: 294.8 °C; ^{1}H NMR (400 MHz, DMSO) δ 10.68 (s, 1H), 7.92 (dd, J = 8.8, 2.1 Hz, 2H), 7.82 (dd, J = 8.6, 2.3 Hz, 2H), 7.35 (s, 1H), 7.21 (dd, J = 8.2, 2.0 Hz, 1H), 7.08 (s, 1H), 6.78 (dd, J = 8.1, 2.8 Hz, 1H); ^{13}C NMR (100 MHz, DMSO) δ 167.67, 162.29, 151.16, 145.83, 145.66,

145.46, 131.21, 126.66, 123.34, 117.63, 116.29, 116.21, 114.00, 101.47; LRMS (ESI) *m/z*: 329.1 $[M+H]^+$; HRMS (ESI) *m/z*: Calcd. for $[M+H]^+$ $C_{16}H_{13}N_2O_4S$: 329.0591; found: 329.0591.

*4.15.18. 3-((4-(3-Hydroxy-4-methoxyphenyl)thiazol-2-yl)amino) benzoic acid (**20c**)*

MP: 268.7 °C; ^{1}H NMR (400 MHz, DMSO) δ 10.39 (s, 1H), 9.05 (s, 1H), 8.22 (s, 1H), 8.04 (dd, *J* = 8.1, 1.2 Hz, 1H), 7.54 (d, *J* = 7.7 Hz, 1H), 7.42 (t, *J* = 7.9 Hz, 1H), 7.37–7.32 (m, 2H), 7.09 (s, 1H), 6.94 (d, *J* = 9.0 Hz, 1H), 3.79 (s, 3H); ^{13}C NMR (100 MHz, DMSO) δ 163.10, 159.70, 150.64, 147.91, 146.84, 141.68, 134.44, 132.51, 129.32, 128.25, 122.54, 120.39, 117.41, 113.64, 112.55, 101.48, 56.09; LRMS (ESI) *m/z*: 343.1 $[M+H]^+$; HRMS (ESI) *m/z*: Calcd. for $[M+H]^+$ $C_{17}H_{15}N_2O_4S$: 343.0747; found: 343.0749.

*4.15.19. 4-((4-(3-Hydroxy-4-methoxyphenyl)thiazol-2-yl)amino) benzoic acid (**20d**)*

MP: 264.4 °C; ^{1}H NMR (400 MHz, DMSO) δ 10.66 (s, 1H), 9.11 (s, 1H), 7.93 (d, *J* = 8.8 Hz, 2H), 7.82 (d, *J* = 8.8 Hz, 2H), 7.40 (d, *J* = 2.1 Hz, 1H), 7.33 (dd, *J* = 8.3, 2.1 Hz, 1H), 7.16 (s, 1H), 6.95 (d, *J* = 8.5 Hz, 1H), 3.79 (s, 3H); ^{13}C NMR (100 MHz, DMSO) δ 162.46, 150.71, 147.96, 146.88, 145.19, 131.16, 128.08, 117.34, 116.25, 113.76, 112.69, 102.29, 56.09; LRMS (ESI) *m/z*: 343.1 $[M+H]^+$; HRMS (ESI) *m/z*: Calcd. for $[M+H]^+$ $C_{17}H_{15}N_2O_4S$: 343.0747; found: 343.0749.

*4.15.20. 3-((4-(4-Hydroxy-3-methoxyphenyl)thiazol-2-yl)amino) benzoic acid (**20e**)*

MP: 258.1 °C; ^{1}H NMR (400 MHz, DMSO) δ 10.43 (s, 1H), 8.73 (s, 1H), 7.72 (d, *J* = 8.0 Hz, 1H), 7.57–7.51 (m, 2H), 7.44 (t, *J* = 7.9 Hz, 1H), 7.35 (dd, *J* = 8.2, 1.9 Hz, 1H), 7.17 (s, 1H), 6.80 (d, *J* = 8.2 Hz, 1H), 3.86 (s, 3H); ^{13}C NMR (100 MHz, DMSO) δ 162.88, 150.80, 148.03, 146.81, 141.76, 129.33, 126.75, 122.37, 120.75, 118.81, 117.89, 115.99, 110.34, 100.89, 56.04; LRMS (ESI) *m/z*: 343.1 $[M+H]^+$; HRMS (ESI) *m/z*: Calcd. for $[M+H]^+$ $C_{17}H_{15}N_2O_4S$: 343.0747; found: 343.0745.

*4.15.21. 4-((4-(4-Hydroxy-3-methoxyphenyl)thiazol-2-yl)amino) benzoic acid (**20f**)*

MP: 263.8 °C; ^{1}H NMR (400 MHz, DMSO) δ 10.65 (s, 1H), 9.17 (s, 1H), 7.93 (d, *J* = 8.9 Hz, 2H), 7.81 (d, *J* = 8.9 Hz, 2H), 7.46 (d, *J* = 2.0 Hz, 1H), 7.39 (dd, *J* = 8.1, 2.0 Hz, 1H), 7.24 (s, 1H), 6.83 (d, *J* = 8.2 Hz, 1H), 3.86 (s, 3H).; ^{13}C NMR (100 MHz, DMSO) δ 167.78, 162.37, 151.02, 148.08, 147.01, 145.38, 131.28, 126.62, 123.48, 119.26, 116.29, 116.03, 110.32, 101.83, 56.09; LRMS (ESI) *m/z*: 343.1 $[M+H]^+$; HRMS (ESI) *m/z*: Calcd. for $[M+H]^+$ $C_{17}H_{15}N_2O_4S$: 343.0747; found: 343.0747.

*4.15.22. 3-((4-(3-Fluoro-4-hydroxyphenyl)thiazol-2-yl)amino) benzoic acid (**20g**)*

MP: 293.5 °C; ^{1}H NMR (400 MHz, DMSO) δ 10.46 (s, 1H), 8.46 (s, 1H), 7.93 (d, *J* = 8.0 Hz, 1H), 7.70 (dd, *J* = 2.0, 2.0 Hz, 1H), 7.59 (d, *J* = 8.4 Hz, 1H), 7.53 (d, *J* = 8.0, 1H), 7.53 (d, *J* = 8.0, 1H), 7.47 (t, *J* = 8.0 Hz, 1H), 7.25 (s, 1H), 6.99 (t, *J* = 8.8 Hz, 1H); ^{13}C NMR (100 MHz, DMSO) δ 163.16, 152.67, 150.29, 149.58, 145.08, 144.96, 141.69, 129.51, 127.06, 127.00, 122.38, 120.81, 118.25, 118.04, 113.97, 113.77, 102.04; LRMS (ESI) *m/z*: 331.1 $[M+H]^+$; HRMS (ESI) *m/z*: Calcd. for $[M+H]^+$ $C_{16}H_{12}FN_2O_3S$: 331.0547; found: 331.0548.

*4.15.23. 4-((4-(3-Fluoro-4-hydroxyphenyl)thiazol-2-yl)amino) benzoic acid (**20h**)*

MP: 290.2 °C; ^{1}H NMR (400 MHz, DMSO) δ 10.66 (s, 1H), 7.93 (d, *J* = 8.8 Hz, 2H), 7.80 (d, *J* = 8.8 Hz, 2H), 7.68 (dd, *J* = 12.5, 1.9 Hz, 1H), 7.60 (dd, *J* = 8.4, 1.5 Hz, 1H), 7.30 (s, 1H), 7.01 (t, *J* = 8.8 Hz, 1H); ^{13}C NMR (100 MHz, DMSO) δ 163.16, 152.67, 150.29, 149.58, 145.02 (d, *J* = 12 Hz), 141.69, 129.51, 127.03 (d, *J* = 6 Hz), 122.38, 120.81, 118.15 (d, *J* = 21 Hz), 113.87 (d, *J* = 20 Hz), 113.77, 102.04; LRMS (ESI) *m/z*: 331.1 $[M+H]^+$; HRMS (ESI) *m/z*: Calcd. for $[M+H]^+$ $C_{16}H_{12}FN_2O_3S$: 331.0547; found: 331.0549.

*4.15.24. 3-((4-(3-Chloro-4-hydroxyphenyl)thiazol-2-yl)amino) benzoic acid (**20i**)*

MP: 269.0 °C; ^{1}H NMR (400 MHz, DMSO) δ 8.50 (s, 1H), 7.92–7.89 (m, 2H), 7.43 (dd, *J* = 2.0, 2.0 Hz, 1H), 7.53 (d, *J* = 8.0 Hz, 1H), 7.46 (t, *J* = 7.6, 1H), 7.27 (s, 1H), 7.03 (d, *J* = 8.8, 1H); ^{13}C NMR (100 MHz, DMSO) δ 167.81, 163.31, 153.27, 148.91, 141.76, 132.00, 129.63, 127.56, 127.22, 125.83, 122.45, 121.36, 120.35, 118.14, 117.23, 102.10; LRMS (ESI) *m/z*: 347.0 $[M+H]^+$; HRMS (ESI) *m/z*: Calcd. for $[M+H]^+$ $C_{16}H_{12}ClN_2O_3S$: 347.0252; found: 347.0252.

*4.15.25. 4-((4-(3-Chloro-4-hydroxyphenyl)thiazol-2-yl)amino) benzoic acid (**20j**)*

MP: 294.6 °C; ^{1}H NMR (400 MHz, DMSO) δ 10.75 (s, 1H), 7.93 (d, *J* = 8.7 Hz, 2H), 7.88 (d, *J* = 2.1 Hz, 1H), 7.80 (d, *J* = 8.8 Hz, 2H), 7.74 (dd, *J* = 8.4, 2.1 Hz, 1H), 7.32 (s, 1H), 7.05 (dd, *J* = 8.5, 2.3 Hz, 1H); ^{13}C NMR (100 MHz, DMSO) δ 167.62, 162.71, 153.22, 149.52, 145.30, 131.29, 127.45, 127.40, 126.16, 123.48, 120.38, 117.23, 116.37, 102.88; LRMS (ESI) *m/z*: 347.0 $[M+H]^+$; HRMS (ESI) *m/z*: Calcd. for $[M+H]^+$ $C_{16}H_{12}ClN_2O_3S$: 347.0252; found: 347.0255.

*4.15.26. 3-((4-(3-Fluoro-4-hydroxyphenyl)thiazol-2-yl)amino) benzonitrile (**20k**)*

MP: 268.4 °C; ^{1}H NMR (400 MHz, DMSO) δ 10.64 (s, 1H), 10.04 (s, 1H), 8.18 (s, 1H), 7.96 (d, *J* = 8.4 Hz, 1H), 7.66 (dd, *J* = 12.7, 2.0 Hz, 1H), 7.59–7.52 (m, 2H), 7.40 (d, *J* = 7.7 Hz, 1H), 7.30 (s, 1H), 7.01 (t, *J* = 8.8 Hz, 1H); ^{13}C NMR (100 MHz, DMSO) δ 162.78, 152.69, 150.30, 149.69, 149.67, 145.10 (d, *J* = 12 Hz), 142.22, 130.90, 126.87 (d, *J* = 7 Hz), 124.88, 122.47 (d, *J* = 3 Hz), 121.71, 119.54 (d, *J* = 7 Hz), 118.34 (d, *J* = 3 Hz), 113.85 (d, *J* = 20 Hz), 112.19, 102.81; LRMs (ESI) *m/z*: 312.1 $[M+H]^+$; HRMS (ESI) *m/z*: Calcd. for $[M+H]^+$ $C_{16}H_{11}FN_3OS$: 312.0601; found: 312.0603.

*4.15.27. 4-(2-((3-(2H-tetrazol-5-yl)phenyl)amino)thiazol-4-yl)-2-fluorophenol (**20l**)*

MP: 241.3 °C; ^{1}H NMR (400 MHz, DMSO) δ 10.54 (s, 1H), 10.01 (s, 1H), 8.55 (s, 1H), 7.93–7.88 (m, 1H), 7.72 (dd, *J* = 12.7, 1.8 Hz, 1H), 7.62 (d, *J* = 8.4 Hz, 1H), 7.57 (d, *J* = 6.4 Hz, 2H), 7.27 (s, 1H), 7.00 (t, *J* = 8.8 Hz, 1H); ^{13}C NMR (100 MHz, DMSO) δ 162.93 (d, *J* = 32 Hz), 156.61, 152.68, 150.30, 149.64, 145.02 (d, *J* = 12 Hz), 142.38, 130.55, 127.02 (d, *J* = 6 Hz), 125.91, 122.55, 119.6 (d, *J* = 41 Hz), 118.25, 115.47, 113.95 (d, *J* = 20 Hz), 102.30; LRMS (ESI) *m/z*: 355.1 $[M+H]^+$; HRMS (ESI) *m/z*: Calcd. for $[M+H]^+$ $C_{16}H_{12}FN_6OS$: 355.0772; found: 355.0771.

*4.15.28. 3-((4-(3-Fluoro-4-hydroxyphenyl)-5-methylthiazol-2-yl) amino)benzoic acid (**24a**)*

MP: 274.6 °C; ^{1}H NMR (400 MHz, DMSO) δ 10.28 (s, 1H), 8.31 (s, 1H), 7.91–7.81 (m, 1H), 7.50 (d, *J* = 7.7 Hz, 1H), 7.43 (dt, *J* = 15.7, 5.0 Hz, 2H), 7.33 (dd, *J* = 8.4, 1.5 Hz, 1H), 7.02 (t, *J* = 8.8 Hz, 1H), 2.41 (s, 3H); ^{13}C NMR (100 MHz, DMSO) δ 168.07, 159.09, 152.30, 149.91, 144.58 (d, *J* = 12 Hz), 141.85, 132.43, 129.54, 127.29 (d, *J* = 7 Hz), 124.61 (d, *J* = 3 Hz), 122.08, 120.89, 117.98 (d, *J* = 3 Hz), 117.79, 116.05 (d, *J* = 10 Hz), 115.91, 12.39; LRMS (ESI) *m/z*: 345.1 $[M+H]^+$; HRMS (ESI) *m/z*: Calcd. for $[M+H]^+$ $C_{17}H_{14}FN_2O_3S$: 345.0704; found: 345.0704.

*4.15.29. 3-(4-(4-Hydroxy-3-methoxyphenyl)-5-methylthiazol-2-ylamino)benzoic acid (**24b**)*

MP: 264.8 °C; ^{1}H NMR (400 MHz, DMSO) δ 10.29 (s, 1H), 8.54 (s, 1H), 7.70 (dd, *J* = 8.0, 1.3 Hz, 1H), 7.51 (d, *J* = 7.6 Hz, 1H), 7.41 (t, *J* = 7.9 Hz, 1H), 7.31 (d, *J* = 1.9 Hz, 1H), 7.06 (dd, *J* = 8.2, 2.0 Hz, 1H), 6.84 (d, *J* = 8.2 Hz, 1H), 3.83 (s, 3H), 2.42 (s, 3H); ^{13}C NMR (100 MHz,

DMSO) δ 161.97, 150.99, 146.29, 145.83, 141.78, 129.21, 128.27, 125.86, 122.31, 120.62, 118.53, 117.83, 113.85, 104.59, 56.09, 14.54; LRMS (ESI) *m/z*: 357.1 $[M+H]^+$; HRMS (ESI) *m/z*: Calcd. for $[M+H]^+$ $C_{18}H_{17}N_2O_4S$: 357.0904; found: 357.0906.

*4.15.30. 3-(4-(4-Hydroxy-5-methoxy-2-methylphenyl)thiazol-2-ylamino)benzoic acid (**24c**)*

MP: 261.1 °C; ^1H NMR (400 MHz, DMSO) δ 10.45 (s, 1H), 8.60 (s, 1H), 7.72 (d, $J = 8.1$ Hz, 1H), 7.51 (d, $J = 7.7$ Hz, 1H), 7.41 (t, $J = 7.9$ Hz, 1H), 7.31 (s, 1H), 6.87 (s, 1H), 6.68 (s, 1H), 3.80 (s, 3H), 2.36 (s, 3H); ^{13}C NMR (100 MHz, DMSO) δ 168.11, 158.84, 147.80, 146.32, 145.80, 141.98, 132.19, 129.45, 127.05, 122.05, 121.05, 120.86, 117.63, 115.60, 115.02, 112.60, 55.91, 12.51; LRMS (ESI) *m/z*: 357.1 $[M+H]^+$; HRMS (ESI) *m/z*: Calcd. for $[M+H]^+$ $C_{18}H_{17}N_2O_4S$: 357.0904; found: 357.0904.

*4.15.31. 3-((6-Hydroxy-5-methoxy-8H-indeno[1,2-d]thiazol-2-yl)amino)benzoic acid (**27a**)*

MP: 308.4 °C; ^1H NMR (400 MHz, DMSO) δ 10.46 (s, 1H), 8.88 (s, 1H), 8.19–8.12 (m, 2H), 7.53 (dt, $J = 7.6$, 1.3 Hz, 1H), 7.50–7.42 (m, 1H), 7.09 (s, 1H), 6.99 (s, 1H), 3.85 (s, 3H), 3.65 (s, 2H); ^{13}C NMR (100 MHz, DMSO) δ 167.38, 156.91, 147.13, 144.89, 141.74, 138.44, 129.66, 129.48, 122.29, 122.11, 120.98, 118.03, 113.61, 103.00, 56.38, 32.19; LRMS (ESI) *m/z*: 355.1 $[M+H]^+$; HRMS (ESI) *m/z*: Calcd. for $[M+H]^+$ $C_{18}H_{15}N_2O_4S$: 355.0747; found: 355.0745.

*4.15.32. 4-((6-Hydroxy-5-methoxy-8H-indeno[1,2-d]thiazol-2-yl)amino)benzoic acid (**27b**)*

MP: 316.9 °C; ^1H NMR (400 MHz, DMSO) δ 10.69 (s, 1H), 8.87 (s, 1H), 7.92 (d, $J = 8.9$ Hz, 2H), 7.82 (d, $J = 8.9$ Hz, 2H), 7.16 (s, 1H), 7.00 (s, 1H), 3.86 (s, 3H), 3.66 (s, 2H); ^{13}C NMR (100 MHz, DMSO) δ 167.64, 166.67, 157.06, 147.19, 145.35, 144.94, 138.38, 131.25, 129.36, 123.28, 122.90, 116.37, 113.56, 103.12, 56.41, 32.21; LRMS (ESI) *m/z*: 355.1 $[M+H]^+$; HRMS (ESI) *m/z*: Calcd. for $[M+H]^+$ $C_{18}H_{15}N_2O_4S$: 355.0747; found: 355.0750.

Acknowledgment

This research was supported by Animal Disease Management Technology Development Program, Ministry of Agriculture, Food and Rural Affairs.

Appendix A. Supplementary data

Supplementary data related to this article can be found at http://dx.doi.org/10.1016/j.ejmech.2015.08.020.

References

[1] Pereira, H.G. Acad. Press, N. Y. N. Y., 1981, pp. 333–363.
[2] F. Sobrino, M. Sai, M.A. Jimenez-Clavero, J.I. Nunez, M.F. Rosas, Vet. Res. 32 (2001) 1–30.
[3] W. Pengyan, R. Yan, G. Zhiru, F.C. Chuang, Virol. J. 5 (2008) 86.
[4] H.L. Bachrach, Annu. Rev. Microbiol. 22 (1968) 201–244.
[5] E. Domingo, C. Escarmis, E. Baranowski, C.M. Ruiz-Jarabo, E. Carrillo, J.I. Nunez, F. Sobrino, Virus Res. 91 (2003) 47–63.
[6] N.J. Knowles, A.R. Samuel, Virus Res. 91 (2003) 65–80.
[7] M.J. Grubman, B.H. Robertson, D.O. Morgan, D.M. Moore, D. Dowbenko, J. Virol. 50 (1984) 579–586.
[8] B.H. Robertson, M.J. Grubman, G.N. Weddell, D.M. Moore, J.D. Welsh, T. Fischer, D.J. Dowbenko, D.G. Yansura, B. Small, D.G. Kleid, J. Virol. 54 (1985) 651–660.
[9] M.J. Grubman, B. Baxt, Clin. Microbiol. Rev. 17 (2004) 465–493.
[10] W. Klump, O. Marquardt, P.H. Hofschneider, Proc. Natl. Acad. Sci. 81 (1984) 3351–3355.
[11] M.D. Ryan, G.J. Belsham, A.M. King, Virology 173 (1989) 35–45.
[12] a K.M. Cowan, J.H. Graves, Virology 30 (1966) 528–540;
b P.A. Lowe, F. Brown, Virology 111 (1981) 23–32;
c J.F. Newman, B. Cartwright, T.R. Doel, F. Brown, J. Gen. Virol. 45 (1979) 497–507;
d P.A. Lowe, F. Brown, Virology 111 (1981) 23–32;
e B.H. Robertson, D.O. Morgan, D.M. Moore, M.J. Grubman, J. Card, T. Fischer, G. Weddell, D. Dowbenko, D. Yansura, Virology 126 (1983) 614–623.
[13] D.J. Paton, J.F. Valarcher, I. Bergmann, O.G. Matlho, V.M. Zakharov, E.L. Palma, G.R. Thomson, Revue Sci. Tech. 24 (2005) 981–993.
[14] M.J. Grubman, Biologicals 33 (2005) 227–234.
[15] W.T. Golde, J.M. Pacheco, H. Duque, T. Doel, B. Penfold, G.S. Ferman, D.R. Gregg, L.L. Rodriguez, Vaccine 23 (2005) 5775–5782.
[16] S. Sierra, M. Davila, P.R. Lowenstein, E. Domingo, J. Virol. 74 (2000) 8316–8323.
[17] N. Pariente, S. Sierra, P.R. Lowenstein, E. Domingo, J. Virol. 75 (2001) 9723–9730.
[18] B. Rada, M. Dragun, Ann. N. Y. Acad. Sci. 284 (1977) 410–417.
[19] J.C. de la Torre, B. Alarcon, E. Martinez-Salas, L. Carrasco, E. Domingo, J. Virol. 61 (1987) 235–255.
[20] S.-M. Kim, J.-H. Park, K.-N. Lee, S.-K. Kim, Y.-J. Ko, H.-S. Lee, I.-S. Cho, Antivir. Res. 96 (2012) 213–220.
[21] N. Goris, A. De Palma, J.F. Toussaint, I. Musch, J. Neyts, K. De Clercq, Antivir. Res. 73 (2007) 61–68.
[22] D.J. Lefebvre, A.R. De Vleeschauwer, N. Goris, D. Kollanur, A. Billiet, L. Murao, J. Neyts, K. De Clercq, Transbound. Emerg. Dis. 6 (2014) e89–91.
[23] Y. Furuta, K. Takahashi, K. Shiraki, K. Sakamoto, D.F. Smee, D.L. Barnard, B.L. Gowen, J.G. Julander, J.D. Morrey, Antivir. Res. 82 (2009) 95–102.
[24] K. Sakamoto, S. Ohashi, R. Yamazoe, K. Takahashi, Y. Furuta, FAO Report of the European Commission for the Control of Foot-and-mouth Disease, 2006, pp. 414–420 (available at: www.fao.org/ag/againfo/commissions/docs/research_group/paphos/App64.pdf.
[25] A.R. De Vleeschauwer, D.J. Lefebvre, T. Willems, G. Paul, A. Billiet, L.E. Murao, J. Neyts, N. Goris, K. De Clercq, Transbound. Emerg. Dis. (2014), http://dx.doi.org/10.1111/tbed.12255.
[26] R.C. Durk, K. Singh, C.A. Cornelison, D.K. Rai, K.B. Matzek, M.D. Leslie, E. Schafer, B. Marchand, A. Adedeji, E. Michailidis, C.A. Dorst, J. Moran, C. Pautler, L.L. Rodriguez, M.A. McIntosh, E. Rieder, S.G. Sarafianos, PloS one 5 (2010) e15049.
[27] D.K. Rai, E.A. Schafer, K. Singh, M.A. McIntosh, S.G. Sarafianos, E. Rieder, Antivir. Res. 98 (2013) 380–385.
[28] N.R.R. Rosell, L. Mokhlesi, N.E. Milton, T.R. Sweeney, P.A. Zunszain, S. Curry, R.J. Leatherbarrow, Núria R. Roqué Rosella, Bioorg. Med. Chem. Lett. 24 (2014) 490–494.
[29] G. Campagnola, P. Gong, O.B. Peersen, Antivir. Res. 91 (2011) 241–251.
[30] J.M. Singh, J. Med. Chem. 13 (1970) 1018.
[31] K.K. Roy, S. Singh, S.K. Sharma, R. Srivastava, V. Chaturvedi, A.K. Saxena, Bioorg. Med. Chem. Lett. 21 (2011) 5589–5593.
[32] J.B. Baell, G.A. Holloway, J. Med. Chem. 53 (2010) 2719–2740.
[33] 3- or 4-substitutied inversed carboxamide such as $CONH_2$, CONHMe on B ring were inactive to enzyme inhibition.
[34] H.-J. Böhm, D. Banner, S. Bendels, M. Kansy, B. Kuhn, K. Müller, U. Obst-Sander, M. Stahl, ChemBioChem 5 (2004) 637–643.
[35] S.M. Kim, K.N. Lee, S.J. Lee, Y.J. Ko, H.S. Lee, C.H. Kweon, H.S. Kim, J.H. Park, Antivir. Res. 87 (2010) 307–317.